Interlayer Self-Diffusion on Stepped Pt(111)

Peter J. Feibelman

Sandia National Laboratories, Albuquerque, New Mexico 87185-1413

(Received 4 March 1998)

Challenging our understanding of epitaxy on clean and O-precovered Pt(111), the *ab initio* Schwoebel barrier calculated for downward self-diffusion across *A*-type steps on Pt(111) is only $E^S(A) \approx 0.02$ eV. Geometric arguments explain why $E^S(B)$, the Schwoebel barrier at *B*-type steps, is more than an order of magnitude larger than $E^S(A)$. [S0031-9007(98)06485-0]

PACS numbers: 68.35.Bs, 68.35.Fx, 68.45.Da, 81.15.–z

The time evolution of a surface's morphology is governed by energetic barriers to diffusion of its constituents. Modern computer power and total-energy algorithms make it possible to estimate the relevant bottlenecks accurately from first principles. This means we can now lay the groundwork for reliable simulations of materials growth, aging, and failure, and expect to gain meaningful, atomic-level insight into these important processes.

Because an evolving surface is inherently imperfect, the barriers that need to be computed correspond to atomic displacements not only on terraces but also near steps, kinks, vacancies, and impurities. The recent scanning tunneling microscopy study of Pt epitaxy on Pt(111) by Esch *et al.* [1] provides the dramatic example on which the present work is focused: Between 300 and 400 K, Pt deposition on the clean surface produces three-dimensional, pyramidal islands. But if the surface is O precovered, then growth is virtually ideal layer by layer. According to Ref. [1], it is by assisting downward transport of Pt adatoms at island boundaries that O inhibits island nucleation on preexisting islands, and thus eliminates pyramid formation.

To confirm this notion theoretically, and to understand its mechanism, it is first necessary to study interlayer transport on O-free, stepped Pt(111). I have therefore performed *ab initio* barrier calculations for downward diffusion of Pt adatoms at steps on Pt(111), and here report the surprising results.

The most important of these is that E_A, the barrier to self-diffusion down a (100) microfacet or *A-type* step, is only $\sim$20 meV bigger than E_T, the self-diffusion barrier on Pt(111). Thus, $E^S(A) \equiv E_A - E_T$, the so-called Schwoebel barrier [2] that impedes transport down *A*-type steps, is small even in the absence of O.

This result conflicts with the finding of Ref. [1] that pyramid edges on clean Pt(111) at 400 K are mainly *A* steps, and with the contention that O-assisted interlayer transport is what promotes layer-by-layer epitaxy. Since pyramids grow when islands *stack* instead of dissipating onto lower terraces, they should be bounded by edges that present large, not minute Schwoebel barriers; and as long as *A* steps form a substantial part of each island's boundary in epitaxy, as in Ref. [1], transport of Pt adatoms off islands will be facile without adsorbed-O's assistance. (Happily, new experiments show that eliminating CO contamination eliminates the conflict [3].)

A second surprising theoretical result is that E_B, the downward self-diffusion barrier across "*B*-type" or (111)-microfacet steps, is not $\sim$0.02 but 0.35 eV bigger than E_T. *Thus the B-step Schwoebel barrier,* $E^S(B) \equiv E_B - E_T$*, is more than an order of magnitude larger than* $E^S(A)$. This contrast on Pt(111), though finally not so mysterious, is quite unexpected. The only previous *ab initio* study of self-diffusion on a stepped, close-packed metal surface, Al(111), yielded a much weaker anisotropy [4].

For both A- and B-type steps the lowest-barrier, downward-transport mechanism is concerted substitution [2]: The upper-terrace adatom implants in the step edge, while a step-edge atom emerges onto the lower terrace (see Figs. 1 and 2). The key fact underlying the barrier anisotropy is that, along the minimum-energy path, the latter atom is guided by its lower-terrace neighbors. The result is that at a *B* step the emerging atom passes through a transition configuration where it is three coordinated [Fig. 2(b)], while, at an *A* step, the emergent atom never has fewer than four near neighbors [Fig. 1(b)]. This difference is presumably more important for Pt than for Al because Al is trivalent.

Though this is not the first theoretical effort aimed at simulating the morphology of growing Pt(111) [5], when it comes to diffusion across steps, it *is* the first based on *ab initio* electronic structure. This distinction is more important than anticipated—the relative magnitudes of the first-principles Schwoebel barriers *differ qualitatively* from the semiempirical estimates used in growth simulations until now [5].

The results reported here, based on the local density approximation (LDA) [6], were obtained using the efficient and accurate total-energy and molecular-dynamics package, VASP (Vienna *ab initio* simulation package) [7–9], its corresponding ultrasoft-pseudopotential data base, and, to account for exchange and correlation, the Ceperley-Alder potential [10]. Though plane-wave calculations for *d*-electron metals typically require unwieldy basis sets, use of an ultrasoft Pt pseudopotential with a 14 Ry basis cutoff assures absolute convergence of total energies to $\sim$10 meV. To accelerate electronic relaxation, I use the

 0031-9007/98/81(1)/168(4)$15.00

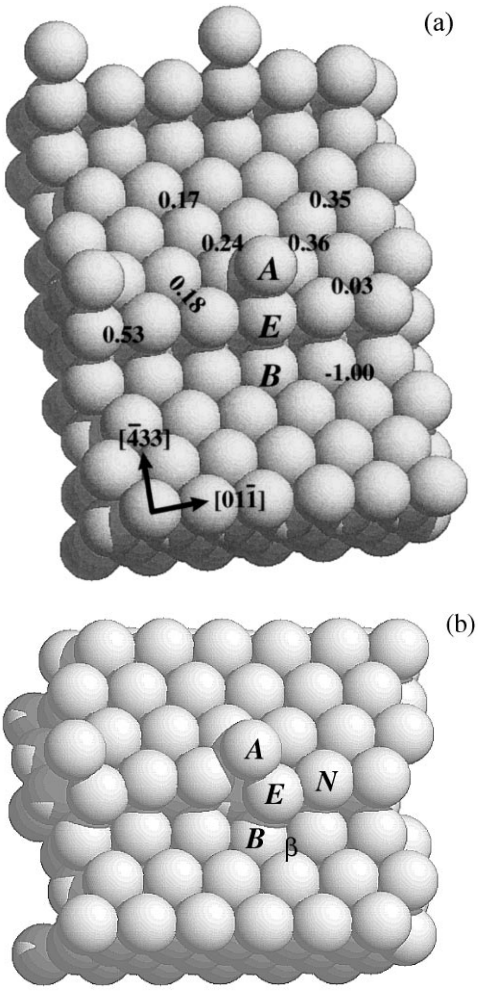

FIG. 1. (a) Initial and (b) downward-diffusion barrier geometries for the *A*-type step of Pt(322). The adatom, the emergent edge atom (destined for site β), and its nearest neighbors in the step edge and at the step bottom are labeled *A*, *E*, *N*, and *B*. Calculated energies (in eV) shown at various adatom sites are defined relative to the configuration illustrated in panel (a).

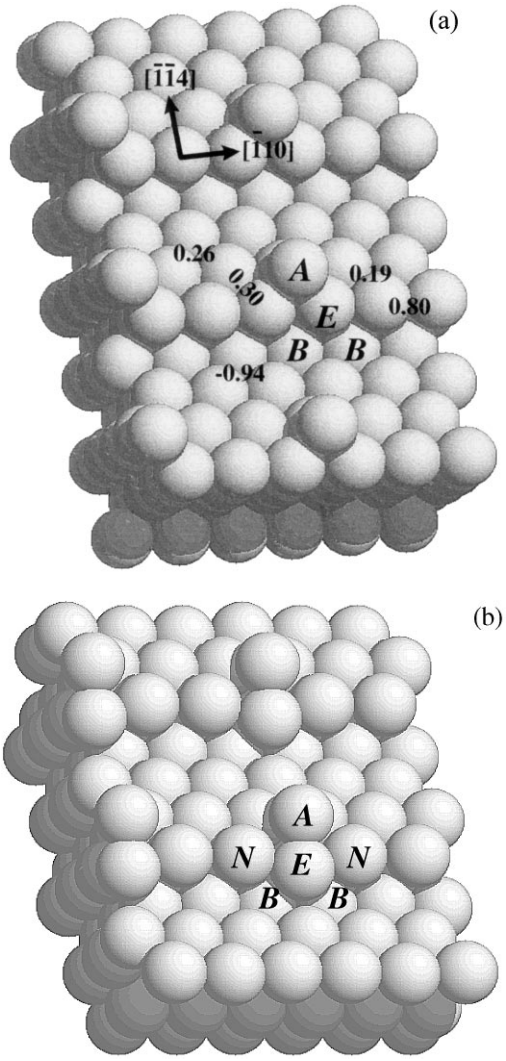

FIG. 2. (a) Initial and (b) downward-diffusion barrier geometries for the *B*-type step of Pt(221). The adatom, the emergent edge atom, and its nearest neighbors in the step edge and at the step bottom are labeled *A*, *E*, *N*, and *B*. Energies (in eV) shown at various adatom sites are defined relative to the configuration illustrated in panel (a).

Fermi-level smearing approach of Methfessel and Paxton [11], with a Gaussian width of 0.2 eV. I optimize geometries until the forces on all unconstrained atoms are smaller than 0.03 eV/Å.

To obtain baseline diffusion energetics for Pt on Pt(111), I relax $\frac{1}{12}$ ML Pt on a six-layer Pt(111) slab in a $3 \times 2\sqrt{3}$ supercell, placing the Pt adatoms first in fcc, ten in hcp hollows, and finally finding the barrier site between them. In these calculations, I fix the lower three layers of the film in the bulk, LDA atomic arrangement (LDA lattice parameter = 3.911 Å) and allow the remaining atoms to relax. To determine an adequate surface Brillouin zone (SBZ) sample, I perform calculations using four special k points in the full SBZ, then assess convergence using a sixteen-**k** sample. The corrugation of the adatom potential energy on Pt(111) is apparently accurate to 0.01 eV with four **k**'s.

The Pt(111) calculations yield a 0.29 eV Pt diffusion barrier on Pt(111), in good agreement with the values 0.25 and 0.26 eV that emerge from field ion [12] and scanning tunneling microscope [13] studies. Earlier calculations [12,14,15], not based on ultrasoft pseudopotentials, produced somewhat higher values. The best converged [15] yields 0.33 ± 0.03 eV, consistent with the present result.

The Pt adatom preference for fcc sites in the present and earlier *ab initio* calculations [12,14,15] agrees with field ion microscope (FIM) data [12,16]. The fcc-hcp binding-energy difference is known experimentally to be >60 meV [16]. The present result, 0.21 eV, is in reasonable agreement with the LDA binding difference (0.17 ± 0.03) eV obtained for a smaller supercell and thinner slab [15].

To estimate diffusion barriers down *A*- and *B*-type steps, I compute the energetics of 3×1 arrangements of Pt adatoms on 20-layer-Pt(322) and 18-layer-Pt(221) slabs (see Figs. 1 and 2), in each case fixing the lower five

layers in their bulk positions as I search for the configurations that correspond to adatom diffusion barriers. Based on the Pt(111) results discussed above, and spot checks for the vicinal surfaces using 36 **k**'s, I sample the (3×1) slabs' SBZs with sixteen **k** vectors.

Key constraints on Pt diffusion across steps on Pt(111), first discussed by Villarba and Jonsson (VJ) [5(a)], apply equally in their semiempirical and the present *ab initio* description of the process. The first constraint is imposed by the high energy of two-coordinated Pt atoms. The result is that at both A and B steps, Pt hopping over the step edge is energetically unfavorable compared to concerted substitutional diffusion (CSD). The present calculations imply that Pt hopping over an A-type step on Pt(111) is 0.22 eV more costly than CSD, and, at a B step, 0.16 eV more costly.

In CSD down steps, the key constraint is that the low energy path for E, the emerging step-edge atom, is between not over its lower-terrace neighbors. This fact, as noted by both VJ [5(a)] and SS [4(a)], means that, at an A step, atom E initially prefers not to emerge along a step normal [see Fig. 1(b)]. Instead, it moves more directly toward its final destination [site β in Fig. 1(b)], passing through a four-coordinated configuration, at worst. At a B step, the same constraint means that E *does* initially displace along a normal to the edge, and must pass through a three-coordinated site [see Fig. 2(b)].

Finding the A-step barrier on Pt(322).—To locate the transition geometry for CSD down an A step, it suffices to search a grid encompassing plausible barrier positions, (x_E, y_E), of the emerging step-edge atom (E, in Fig. 1), where the Cartesian axes are $[01\bar{1}]$ and $[\bar{4}33]$. At each (x_E, y_E), I allow z_E, and the x, y, and z coordinates of all of the rest of the atoms in the 3×1 cell [17] to optimize, then compute the x and y components of F, the force on E. The barrier, or saddle point, is where F vanishes while the determinant $dF_x/dx_E\, dF_y/dy_E - dF_x/dy_E\, dF_y/dx_E < 0$.

The result, illustrated in Fig. 1(b), is that the A-step, downward CSD barrier is only 0.31 eV, just 20 meV larger than the barrier to Pt diffusion by hopping on the flat (111) terrace. Thus, only a small Schwoebel barrier (close to the accuracy limit of the present calculations) hinders downward transport of upper-terrace Pt adatoms. This result, which demands that we reconsider why Pt grows three dimensionally on Pt(111) between 300 and 400 K, is not entirely unexpected. It is, in fact, quite similar to Ref. [4]'s result for CSD on A-stepped Al.

Incidently, the A-step CSD barrier obtained semiempirically by VJ [5(a)], 0.30 eV, is very close to that obtained here. VJ's Schwoebel barrier is nonetheless much higher than 0.02 eV because their terrace-diffusion barrier is unphysically low.

By way of interpretation, VJ contend that the A-step CSD barrier is "big," because to avoid step-bottom atom B, emerging atom E must pass close to edge neighbor N. In fact, it is precisely because $\overline{EN}$ is relatively small that E is effectively four-coordinated in the barrier geometry. According to the *ab initio* calculations, distances $\overline{EN}$ and $\overline{EB}$ both equal $\sim$2.52 Å, about 9% less than the bulk nearest-neighbor separation, 2.77 Å. At the same time, E is 2.61 Å from its other lower-terrace neighbor [blocked from view in Fig. 1(b)], and $\sim$2.44 Å from A. Relatively small values of $\overline{EN}$, $\overline{EB}$, and $\overline{EA}$ are favored for two reasons. The first is the usual "bond-order bond length correlation" [18]. The second is that Pt surfaces are typically under tensile stress, which is relieved when low symmetry allows bonds to shorten [19].

Finding the B-step barrier on Pt(221).—An extensive search for the downward-CSD barrier geometry at a B step again confirms that the emergent step-edge atom is initially guided by its lower-terrace neighbors. A consequence, cf. Fig. 2(b), is symmetry of the transition geometry under reflection in a y-z plane (where x, y, and z coordinates lie along $[\bar{1}10]$, $[\bar{1}\bar{1}4]$, and $[221]$). Although this symmetry suggests that to find the barrier one can simply drag the y coordinate of atom E in the y direction, looking for a maximum in the energy, this simple procedure fails. Instead of a smooth curve with a maximum where its slope vanishes, one finds that F_y vs y has two concave-upwards segments meeting at a cusp. The reason is that, on either side of the cusp, other coordinates of the many-atom system relax differently.

Again, therefore, a two-dimensional grid search is required. In the present case, I fix the y coordinates of atom E, and of its immediate step-edge neighbors N. The upshot is a transition geometry [see Fig. 2(b)] in which adatom A has moved to a position near the hcp hollow behind E. At the same time, edge neighbors N, also trailing E, have fallen somewhat behind it.

The calculated barrier is 0.64 eV. Thus, downward transport at a B-type step requires 0.35 eV more than diffusion on the flat Pt(111) terrace, and at low T, CSD is much less probable at a B-type than at an A-type step.

Why is downward diffusion so much more costly at a B-type as against an A-type step? Neighbor counting provides a compelling clue. At the B-step saddle, illustrated in Fig. 2(b), emerging atom E has *only three* near neighbors, adatom A and bottom atoms B. That is, while $\overline{EA}$ and $\overline{EB}$ equal 2.44 and 2.55 Å, E's next-nearest neighbors, atoms N, are 2.80 Å distant. In the A-step transition geometry, as detailed above, the emergent atom has *four* near neighbors.

Another difference between diffusion processes at A- and B-type steps, also favoring A-type, is worth bearing in mind: As illustrated in Figs. 1 and 2, in both cases, the adatom moves along the step from an initial edge-adjacent fcc hollow to a position near an hcp site in the transition geometry. But as the energies shown in Figs. 1(a) and 2(a) imply, adatom displacement along the A-step edge is more facile than along a B step. The energy surface is more corrugated along the B step because the advantages of being in an fcc hollow, and of being coordinated to (and thus passivating) two step-edge atoms, are in phase.

Adjacent to an *A* step, they are not. There, an adatom can *either* reside in an fcc hollow and have one step-edge neighbor, as in Fig. 1(a), *or* it can occupy an hcp site and have two. This is why the fcc-hcp binding difference is only 0.03 eV along an *A* step, but 0.19 eV at a *B* step, and presumably why the barriers to move along *A* and *B* steps are 0.18 vs 0.30 eV.

Having computed and interpreted downward-CSD barriers at steps on Pt(111), I now wish to compare to the experiment and to other theoretical work. Based on FIM observations, Ref. [16] reports that Pt atoms adsorbed at the tops of island edges on Pt(111) only incorporate into the edges somewhat above 130 K. Whether this observation is consistent with a low barrier to CSD at *A* steps requires detailed structural information not provided in Ref. [16], e.g., whether the adatom incorporation occurs at kinks, corners, or at *A*-type steps.

The main point of Ref. [16] is that Pt adatoms on islands avoid a zone 2–3 nearest-neighbor spacings wide, starting one spacing inside the island boundary. The (5-atomic-row wide) terraces on the Pt(322) slab studied here are too narrow to make a detailed comparison with this observation. Nonetheless [see Fig. 1(a)] adatom binding energies on Pt(322) do not monotonically increase as one moves onto the upper terrace from the step edge, but rather, show a maximum.

Concerning attempts to account for the epitaxial-growth morphology of Pt(111) based on semiempirical [5(a)] or on data-fit [5(b)] energetics, Table I shows that this is an unlikely route to lasting, transferable interpretation. Despite some coincidences in barrier and site-occupation energies, the semiempirical results bear no systematic resemblance to those of the *ab initio* calculations.

The surprisingly small Schwoebel barrier for *A* steps is the most important kinetic parameter to emerge from the *ab initio* results. Its smallness is hard to reconcile with the suggestion [1] that O acts as a surfactant by assisting interlayer transport. Learning from a contradiction of this nature is virtually impossible if one starts from a theoretical method of questionable accuracy, and completely impossible if one works backward from experiment. New studies [3], attributing the growth-morphology transition of Ref. [1] to CO contamination, underline this caution.

TABLE I. *Ab initio* vs semiempirical activation barriers for self-diffusion on terraces, and down A- and B-type steps on Pt(111). VASP, EAM, and EMT results refer to the present work, the Embedded Atom Method, and Effective Medium Theory, respectively.

Barrier	VASP	EAM[a]	EMT[b]
Hop on (111)-terrace	0.29 eV	0.08 eV	0.16 eV
Exchange down A-step	0.31 eV	0.30 eV	"not low"
Exchange down B-step	0.64 eV	0.18 eV	0.37 eV
Hop down A-step	0.53 eV	not given	0.41 eV
Hop down B-step	0.80 eV	not given	not given

[a]Ref. [5(a)].
[b]Ref. [5(b)].

I thank R. Stumpf and T. Michely for numerous discussions, and the latter and M. Kalff for access to their unpublished results. VASP [7–9] was developed at the Institut für Theoretische Physik of the Technische Universität Wien. This work was supported by the U.S. Department of Energy under Contract No. DE-AC04-94AL85000. Sandia is a multiprogram laboratory operated by Sandia Corporation, a Lockheed-Martin Company, for the U.S. Department of Energy.

[1] S. Esch, M. Hohage, T. Michely, and G. Comsa, Phys. Rev. Lett. **72**, 518 (1994).
[2] R. L. Schwoebel and E. J. Shipsey, J. Appl. Phys. **37**, 3682 (1966); G. Ehrlich and F. G. Hudda, J. Chem. Phys. **44**, 1039 (1966).
[3] M. Kalff, G. Comsa, and T. Michely (unpublished) show that background CO, below its desorption temperature of 400–500 K, is what stabilized the *A*-step-bounded islands and pyramids of Ref. [1], and infer that O simply removed the CO.
[4] R. Stumpf and M. Scheffler [(a) Phys. Rev. B **53**, 4958 (1996); (b) Phys. Rev. Lett. **72**, 254 (1994)] report $E^S(A) = 0.08$ eV and $E^S(B) = 0.06$ eV for self-diffusion on stepped Al(111).
[5] See, e.g., (a) M. Villarba and H. Jonsson, Surf. Sci. **317**, 15 (1994); (b) J. Jacobsen, K. W. Jacobsen, P. Stoltze, and J. K. Nørskov, Phys. Rev. Lett. **74**, 2295 (1995).
[6] See *The Theory of the Inhomogeneous Electron Gas*, edited by S. Lundqvist and N. H. March (Plenum, New York, 1983); also, W. E. Pickett, Comput. Phys. Rep. **9**, 115 (1989).
[7] G. Kresse and J. Hafner, Phys. Rev. B **47**, 558 (1993); **49**, 14 251 (1994).
[8] G. Kresse and J. Furthmüller, Comput. Mater. Sci. **6**, 15 (1996).
[9] G. Kresse and J. Furthmüller, Phys. Rev. B **54**, 11 169 (1996).
[10] D. M. Ceperley and B. J. Alder, Phys. Rev. Lett. **45**, 566 (1980), as parametrized by J. Perdew and A. Zunger, Phys. Rev. B **23**, 5048 (1981).
[11] M. Methfessel and A. T. Paxton, Phys. Rev. B **40**, 3616 (1989).
[12] P. J. Feibelman, J. S. Nelson, and G. L. Kellogg, Phys. Rev. B **49**, 10 548 (1994).
[13] M. Bott, M. Hohage, M. Morgenstern, T. Michely, and G. Comsa, Phys. Rev. Lett. **76**, 1304 (1996).
[14] J. J. Mortensen, B. Hammer, O. H. Nielsen, K. W. Jacobsen, and J. K. Nørskov, *Springer Series on Solid State Sciences*, edited by A. Ojiki (Springer, Berlin, 1996), Vol. 121, p. 173.
[15] G. Boisvert, L. J. Lewis, and M. Scheffler, Phys. Rev. B **57**, 1881 (1998).
[16] A. Gölzhäuser and G. Ehrlich, Phys. Rev. Lett. **77**, 1334 (1996).
[17] Except the five bottom layers, as noted above.
[18] L. Pauling, *The Nature of the Chemical Bond* (Cornell University, Ithaca, NY, 1960), 3rd ed.
[19] R. J. Needs, M. J. Godfrey, and M. Mansfield, Surf. Sci. **242**, 215 (1991).